Development 134, 3893-3904 (2007) doi:10.1242/dev.009464

Sulfated glycosaminoglycans are necessary for Nodal signal transmission from the node to the left lateral plate in the mouse embryo

Shinya Oki[1,*], Ryuju Hashimoto[2], Yuko Okui[3], Michael M. Shen[4,†], Eisuke Mekada[5], Hiroki Otani[2], Yukio Saijoh[1,6] and Hiroshi Hamada[1,‡]

Situs-specific organogenesis in the mouse results from leftward fluid flow in the node cavity and subsequent left-sided expression of *Nodal* in the lateral plate mesoderm (LPM). *Nodal* expression at the node is essential for the subsequent asymmetric *Nodal* expression in the left LPM, but the precise role of Nodal produced at the node has remained unknown. We have now investigated how the Nodal signal is transferred from the node to the LPM. Externally supplied Nodal protein failed to signal to the LPM, suggesting that the Nodal signal is transferred to the LPM via an internal route rather than an external one. Transgenic rescue experiments showed that the Nodal co-receptor Cryptic (Cfc1) is required only in the LPM, not at the node, for asymmetric *Nodal* expression in the LPM, indicating that the Nodal signal is not relayed indirectly between the node and LPM. Nodal interacts in vitro with sulfated glycosaminoglycans (GAGs), which are specifically localized to the basement membrane-like structure between the node and LPM in the mouse embryo. Inhibition of sulfated GAG biosynthesis prevents *Nodal* expression in the LPM. These data suggest that Nodal produced at the node might travel directly to the LPM via interaction with sulfated GAGs.

KEY WORDS: Left-right asymmetry, Node, Nodal, Extracellular matrix, Glycosaminoglycan, Mouse

INTRODUCTION

Visceral organs of the mouse exhibit left-right (L-R) asymmetric morphology. Nodal, a secretory protein that belongs to the transforming growth factor-β (TGF-β) superfamily, plays a prominent role in L-R patterning. *Nodal* is expressed at the node of the mouse embryo at embryonic day (E) 8.0 and its expression is subsequently apparent in the left lateral plate mesoderm (LPM) (Hamada et al., 2002; Shiratori and Hamada, 2006). We (Saijoh et al., 2003) and others (Brennan et al., 2002) have shown that mice deficient in *Nodal* expression at the node fail to express *Nodal* in the LPM. However, it has been unclear how Nodal produced at the node directs *Nodal* expression in the LPM. Previous observations that Nodal is able to act over a long distance (Chen and Schier, 2001; Yamamoto et al., 2003) and that *Nodal* expression is regulated by Nodal-responsive enhancers (Norris et al., 2002; Saijoh et al., 2000) suggest that Nodal produced at the node may travel from the node to the LPM. However, direct evidence for such transport of Nodal has proved elusive.

Sulfated glycosaminoglycans (GAGs) have been shown to contribute to morphogen gradient formation (Hacker et al., 2005; Lin, 2004). Sulfated GAGs comprise repeating sulfated disaccharides including *N*-acetylglucosamine and glucuronic or iduronic acid for heparin and heparan sulfate (HS), or *N*-acetylgalactosamine and glucuronic acid for chondroitin sulfate (CS). HS and CS are covalently linked to serine residues of membrane-tethered core proteins, giving rise to heparan sulfate proteoglycans (HSPGs) and chondroitin sulfate proteoglycans, respectively, that are localized to the cell surface or extracellular matrix (ECM). The TGF-β homolog Decapentaplegic (Dpp) acts as an HS-dependent morphogen in anteroposterior patterning of the *Drosophila* wing (Belenkaya et al., 2004); Dpp is thus not able to traverse mutant cells that lack either an HS-polymerizing enzyme (*sulfateless*) or a glypican member of the HSPGs (*dally*). Given that Dpp possesses an affinity for heparin (Groppe et al., 1998), Dpp molecules secreted into the ECM may be immediately captured by sulfated GAGs and transported from one GAG chain to another toward more distally located target cells. Although Nodal is able to exert its action over a long range, the determinants of this signaling range are unknown.

We have now investigated the mechanism by which the Nodal signal is transferred from the node to the LPM in the mouse embryo. Our results support a model in which Nodal produced by the perinodal cells is directly transported to the LPM via sulfated GAGs that are specifically localized to the basement membrane-like structure between the node and the LPM.

[1]Developmental Genetics Group, Graduate School of Frontier Biosciences, Osaka University, and CREST, Japan Science and Technology Corporation (JST), 1-3 Yamada-oka, Suita, Osaka 565-0871, Japan. [2]Department of Developmental Biology and [3]Department of Biosignaling and Radioisotope Experiments, Center for Integrated Research in Science, Faculty of Medicine, Shimane University, 89-1 Enya-cho, Izumo 693-8501, Japan. [4]Center for Advanced Biotechnology and Medicine and Department of Pediatrics, University of Medicine and Dentistry of New Jersey – Robert Wood Johnson Medical School, Piscataway, NJ 08854, USA. [5]Department of Cell Biology, Research Institute for Microbial Diseases, Osaka University, 3-1 Yamadaoka, Suita, Osaka 565-0871, Japan. [6]Department of Neurobiology and Anatomy, Program in Human Molecular Biology and Genetics, and The Eccles Program in Human Molecular Biology and Genetics, University of Utah, Salt Lake City, UT 84112-5330, USA.

*Present address: Department of Developmental Biology, Graduate School of Medical Sciences, Kyushu University, 3-1-1 Maidashi, Higashi-ku, Fukuoka 812-8582, Japan
†Present address: Departments of Medicine and Genetics & Development, Columbia University College of Physicians and Surgeons, Herbert Irving Comprehensive Cancer Center, 1130 St Nicholas Ave, Room 217B, New York, NY 10032, USA
‡Author for correspondence (e-mail: hamada@fbs.osaka-u.ac.jp)

Accepted 20 August 2007

MATERIALS AND METHODS

Search for an LPM-specific enhancer of *Cryptic* and generation of *Cryptic* transgenic mice

Cryptic (*Cfc1*) mutant mice were described previously (Shen et al., 1997; Yan et al., 1999). Enhancer analysis with *lacZ* reporter transgenes (Saijoh et al., 2005) revealed that an 11 kb genomic fragment of *Cryptic* (from –10 to +1 kb relative to the translational initiation site) conferred LPM-specific β-galactosidase activity and was thus designated an LPM-specific enhancer (LPE). The LPE and *hsp68* promoter were linked to *Cryptic* cDNA, an internal ribosomal entry site (IRES) and *lacZ*. Two transgenic lines (#15, #22) that showed LPM-specific expression of this transgene were established in C57BL/6xC3H F1 mice.

To detect the production at the node of Nodal tagged with three copies of the Myc epitope (3×Myc), we generated a transgene containing two copies of the node-specific enhancer (NDE) of *Nodal* (Adachi et al., 1999); the *hsp68* promoter; *Nodal* cDNA containing the nucleotide sequence for the 3×Myc epitope tag (Sigma) positioned four amino acids downstream from the cleavage site; an IRES; and *lacZ*. The 40 amino acid sequence at the NH_2-terminal end of the mature 3×Myc-Nodal protein is thus HHLP*EQKLISEEDLNEQKLISEEDLNEQKLISEEDLG*DRS, with italics indicating the 3×Myc epitope tag. Two transgenic lines (#35, #133) that showed node-specific expression were used in this report.

Whole-mount in situ hybridization

Whole-mount in situ hybridization was performed according to standard procedures with digoxigenin-labeled riboprobes specific for *Nodal* (Lowe et al., 1996), *Lefty1* and *Lefty2* (Meno et al., 1997; Meno et al., 1996), *Pitx2* (Meno et al., 1998), *Gdf1* (Rankin et al., 2000) and *Cryptic* (Shen et al., 1997).

Whole-embryo culture

Injection of expression vectors for Nodal or green fluorescent protein (GFP) and detection of fluorescence were preformed as described previously (Nakamura et al., 2006). In some experiments, embryos were exposed to 15 mM sodium chlorate (Kishida Chemicals), 1 mM *p*-nitrophenyl β-D-xylopyranoside (Sigma) with 0.1% dimethyl sulfoxide as a solubilization carrier, recombinant mouse Nodal (50 μg/ml, R&D Systems) or recombinant human Activin (400 ng/ml, R&D Systems). For protein injection experiments, approximately 0.01 μl culture medium containing 50 μg/ml bovine serum albumin, 50 μg/ml recombinant Nodal or 400 ng/ml Activin was injected with a glass needle (Dramond) and injector (Narishige) into LPM immediately below the endoderm layer. It should be noted that the same concentration was used to bathe the embryos as was used in the injection needle.

Immunofluorescence analysis and transmission electron microscopy

Embryonic day 8.0 ICR or transgenic embryos (with or without subsequent culture) were fixed overnight at 4°C with 4% paraformaldehyde and cryosectioned at a thickness of 6 μm. Immunofluorescence analysis for GAGs and Alcian Blue staining were performed as described previously (Garcia-Garcia and Anderson, 2003; Morriss-Kay and Crutch, 1982), after incubation with heparitinase III (50 mU/ml) or chondroitinase ABC (5 U/ml, both from Seikagaku) at 37°C for overnight under commercially recommended conditions. For immunofluorescence analysis of 3×Myc-tagged Nodal, frozen sections were autoclaved at 121°C for 5 minutes in 10 mM sodium citrate buffer (pH 6.0) before exposure to mouse monoclonal antibodies to Myc (9E10, Santa Cruz Biotechnology) and rabbit polyclonal antibodies either to laminin (Sigma), ZO-1 (Zymed) or β-galactosidase (Zymed); immune complexes were detected with AlexaFluor-conjugated secondary antibodies (Molecular Probes) and nucleus was stained with 4′,6-diamidino-2-phenylindole (DAPI). For immunoenzymatic detection of 3×Myc-Nodal by transmission electron microscopy (TEM), immune complexes were stained with biotinylated antibodies to mouse immunoglobulin G (Jackson Immunolaboratories), horseradish peroxidase-conjugated streptavidin (Vector Laboratories), and *p*-dimethylaminoazobenzene solution containing 60 mM nickel chloride. Sections were first examined with a light microscope and subsequently ultrathin sections were observed with a transmission electron microscope (EM-002B, Topcon) at a magnification of ×1000, ×4000 or ×6000. The details of this procedure were described previously (Hirose et al., 1990).

Interaction between Nodal and sulfated GAGs

Recombinant mouse Nodal (1 μg, R&D Systems) was dissolved in 1 ml of 20 mM HEPES-NaOH (pH 7.2) and incubated overnight at 4°C with 10 μl heparin-sepharose CL-6B (Amersham). The resin was washed three times with the HEPES buffer and then suspended sequentially in 100 μl of elution solution containing various concentrations of NaCl, heparin (porcine intestinal mucosa, Sigma), CS (bovine trachea, Sigma) or HS (porcine intestinal mucosa, Sigma) dissolved in the HEPES buffer. The eluate fractions were boiled in SDS sample buffer containing 0.3 M dithiothreitol and subject to immunoblot analysis with rabbit antiserum specific for the mature domain of mouse Nodal. The amount of eluted Nodal was quantified by comparison with recombinant mouse Nodal as a standard and was normalized relative to the maximal value.

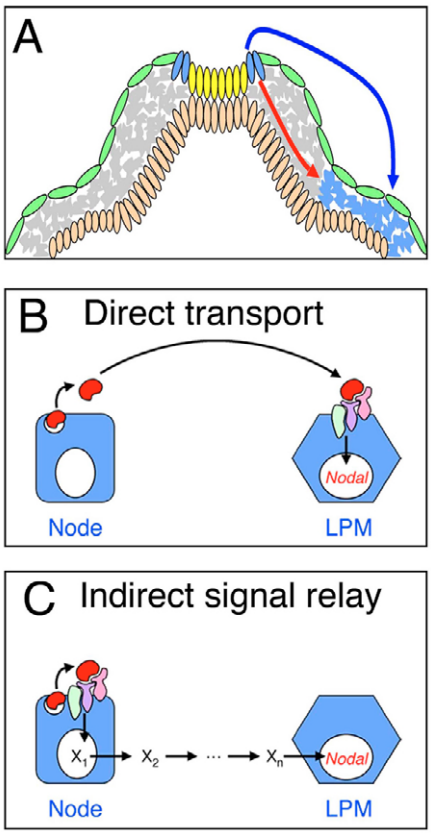

Fig. 1. Schematic representation of possible routes for Nodal signal transmission from the node to LPM in the mouse embryo. (**A**) Schematic transverse section of an E8.2 embryo showing endoderm (green), mesoderm (gray), ectoderm (orange), node (yellow) and *Nodal*-expressing (dark blue) cells. Internal (red arrow) or external (blue arrow) potential routes of Nodal signal transmission are indicated. (**B**,**C**) Two hypothetical mechanisms of Nodal signaling from the node (blue square) to LPM (blue hexagon). Nodal, red; type I and type II Activin receptors, green and purple; Cryptic, pink. In the direct transport model (B), Nodal produced at the node travels directly to LPM, where it is captured by Cryptic and induces *Nodal* expression. In the indirect signal-relay model (C), Nodal produced at the node binds to Cryptic and induces the expression of downstream gene products (X_1, X_2, X_n) that relay the Nodal signal to induce *Nodal* expression in LPM.

RESULTS

The Nodal signal is transmitted from the node to the lateral plate via an internal route

It is most likely that Nodal protein or a signal induced by Nodal is transferred from the node to the LPM. However, the route of this transfer has been unclear. Two different routes are possible (Fig. 1A). (1) An external route, by which Nodal secreted to the apical side of the perinodal crown cells is transported by the leftward fluid flow outside the embryo and is received by the endoderm. The endoderm may transport the received Nodal molecules to the LPM or may generate an unknown signal that is relayed to the LPM. (2) An internal route, by which Nodal is secreted to the basolateral side of the perinodal crown cells and the Nodal signal is then directly or indirectly transmitted to the LPM via the paraxial mesoderm.

To distinguish between these two possibilities, we performed two sets of experiments. If the external route is operative, externally supplied Nodal or Activin would be expected to signal through the endoderm to the LPM and thereby to induce *Nodal* expression bilaterally throughout the LPM (Fig. 2A), as the SELI system (Nakamura et al., 2006) suggests that excessive Nodal signal on the both sides of the LPM would result in bilateral *Nodal* expression in the LPM. We recovered mouse embryos at the one-somite stage and cultured them in medium with or without an excess of recombinant Nodal or Activin protein (which would be way above the concentration of Nodal in the node in vivo) for 7 to 8 hours, until they had developed to the six-somite stage. Under normal culture conditions, *Nodal* expression in the LPM begins at the three-somite stage and has expanded fully by the six-somite stage. However, exogenous Nodal or Activin failed to induce *Nodal* expression in the right LPM (0/10 or 0/9 embryos, respectively; Fig. 2B-D). By contrast, to experimentally generate a situation in which Nodal can signal through the endoderm, we injected them (at the same concentrations as those used for bath application) into the right LPM immediately below the endoderm layer at the one-somite stage (Fig. 2E). The injected embryos were cultured without Nodal or Activin and then examined for *Nodal* expression in the LPM. Local injection of Nodal or Activin induced ectopic *Nodal* expression in the right LPM (11/11 or 2/3 embryos, respectively; Fig. 2G,H), whereas injection of bovine serum albumin failed to do so (0/5 embryos; Fig. 2F). These results thus indicated that the Nodal signal is not transmitted through the endoderm to the LPM, although they do not prove that Nodal can travel through the mesoderm layer. Consistent with the notion, while the endoderm expresses *ALK4* and *ActRIIB*, it fails to express *FoxH1* and *Cryptic* (also known as *Cfc1*), an essential component of Nodal signaling (see Fig. S1 in the supplementary material; data not shown), supporting that the endoderm is not competent to transmit a Nodal signal.

The Nodal signal travels directly from the node to the LPM

Although our results are consistent with the idea that the Nodal signal is transferred from the node to the LPM via the internal route, it remained unclear whether the signal transfer is direct or indirect. Nodal produced at the node may be directly transported to the LPM (Fig. 1B), where it activates *Nodal* expression through the Nodal-responsive enhancers ASE and LSE (Saijoh et al., 2003; Saijoh et al., 2005). Alternatively, Nodal produced at the node may bind to its receptor and co-receptor in the node or paraxial mesoderm and thereby generate a secondary signal that subsequently travels to the LPM and induces *Nodal* expression (Fig. 1C). To distinguish between these possibilities, we focused on Cryptic, a member of the EGF-CFC family of proteins that serves as a co-receptor for Nodal (Shen et al., 1997). *Cryptic* is expressed specifically in the node, LPM and floor plate but not in the paraxial mesoderm (Fig. 3D), and it is the only EGF-CFC family gene that is expressed in those regions of E8.0 embryo; *Cripto* is not expressed at this stage except for in the heart tube (see Fig. S2 in the supplementary material). Furthermore, phosphorylated Smad2/3 is detected in the perinodal cells of the wild-type embryo, but is absent in the *Cryptic*$^{-/-}$ embryo, suggesting that Nodal signal in the node strictly depends on Cryptic (A. Kawasumi and H.H., unpublished). The expression of *Nodal* as well as that of Nodal target genes (*Lefty2*, *Pitx2*) is absent in the left LPM of *Cryptic* knockout mice, in spite of normal expression of *Nodal* at the node (Fig. 3G,K,O) (Yan et al., 1999). If

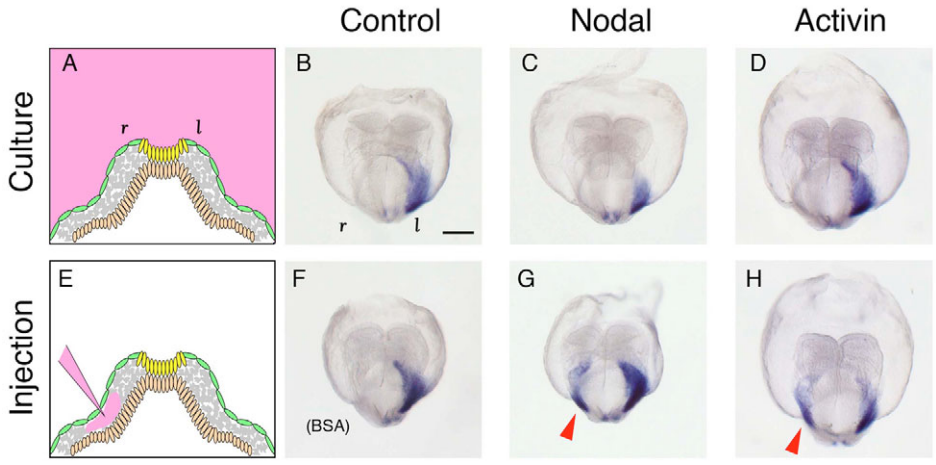

Fig. 2. Unresponsiveness of the endoderm to the Nodal signal. (**A**,**E**) Schematic transverse sections of an E8.0 mouse embryo showing the strategy for culture with (A), or injection of (E), recombinant Nodal or Activin. Recombinant proteins added to the culture medium or injected into the right LPM are colored pink. (**B-D**) In situ hybridization for *Nodal* mRNA in embryos that were recovered at the one-somite stage and cultured in the absence (B) or presence of recombinant Nodal (C) or Activin (D) until they developed to the six-somite stage. (**F-H**) In situ hybridization for *Nodal* mRNA in embryos recovered at the one-somite stage, injected with medium containing bovine serum albumin (F), recombinant Nodal (G) or Activin (H), and cultured to the six-somite stage. Arrowheads indicate ectopic expression of *Nodal* in the right LPM. l, left; r, right. Scale bar: 200 μm.

DEVELOPMENT

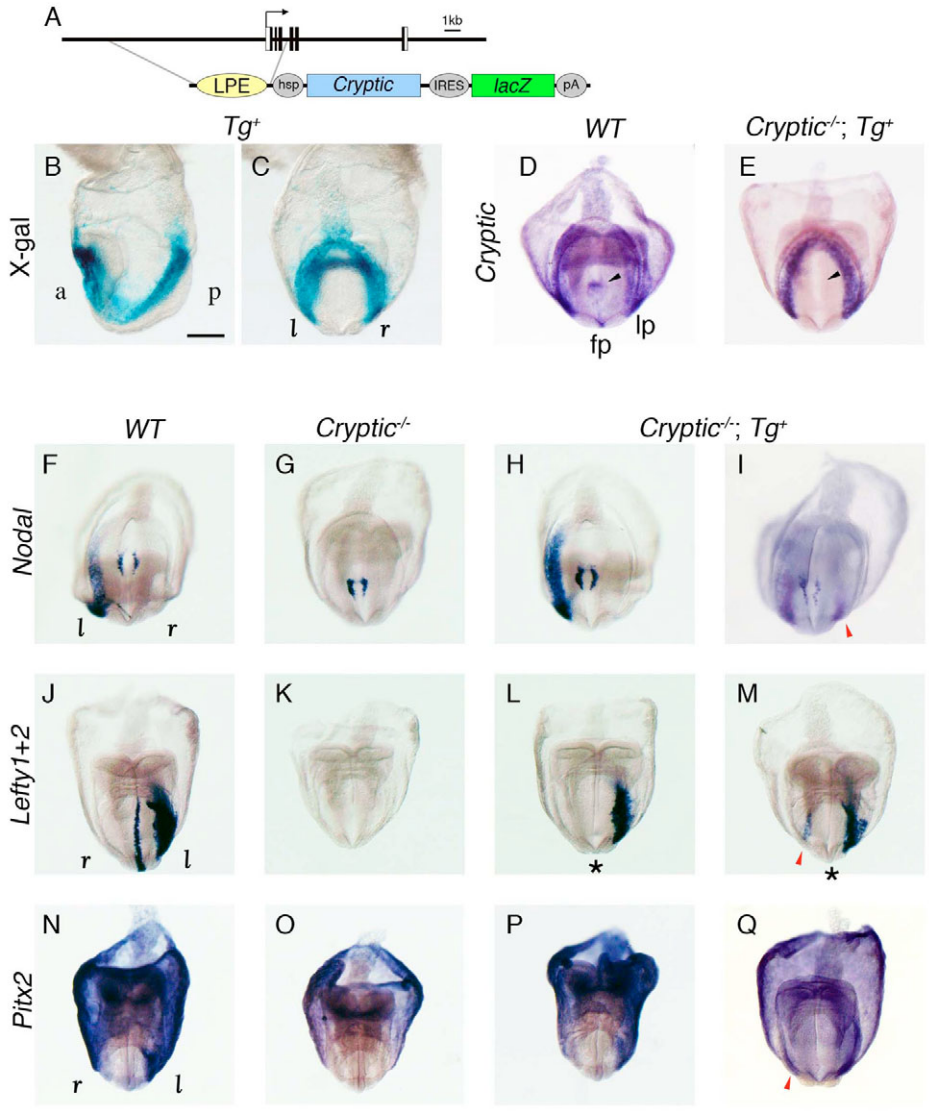

Fig. 3. The Nodal signal is not relayed indirectly between the node and LPM in mouse. (**A**) Schematic representation of a *Cryptic* transgene. An LPE isolated from a *Cryptic* genomic fragment was linked to the *hsp68* promoter, *Cryptic* cDNA, an IRES, *lacZ* and a polyadenylation signal. Black and white boxes represent the open reading frame and untranslated regions, respectively, of *Cryptic*, with the arrow indicating the direction of transcription. (**B**,**C**) An E8.2 embryo harboring the transgene (Tg^+) shows β-galactosidase activity specifically in the LPM. (**D**,**E**) In situ hybridization for *Cryptic* mRNA in wild-type (D) or $Cryptic^{-/-}$; Tg^+ (E) embryos at E8.2. *Cryptic* is expressed only in LPM, not in the node (black arrowhead) or floor plate, of the $Cryptic^{-/-}$; Tg^+ embryo. (**F-Q**) In situ hybridization for *Nodal* (F-I), *Lefty1* and *Lefty2* (J-M) or *Pitx2* (N-Q) transcripts in wild-type (F,J,N), $Cryptic^{-/-}$ (G,K,O), or $Cryptic^{-/-}$; Tg^+ (H,I,L,M,P,Q) embryos at E8.2. The expression of *Nodal*, *Lefty2* and *Pitx2* in LPM is lost in $Cryptic^{-/-}$ embryos (G,K,O), but is rescued by the transgene in $Cryptic^{-/-}$; Tg^+ embryos (H,L,P). Red arrowheads (I,M,Q) indicate ectopic gene expression in the right LPM of $Cryptic^{-/-}$; Tg^+ embryos, which probably results from a defect in the midline barrier (asterisks in L and M). H,I,L,M are all at the five-somite stage. a, anterior; fp, floor plate; lp, LPM; p, posterior; pA, polyadenylation signal. Scale bar: 200 μm.

the indirect signal-relay model is correct, ablation of *Cryptic* expression in the node would be expected to prevent *Nodal* expression in LPM, given that the secondary signal would not be generated in or around the node. Alternatively, if the direct transport model is correct, ablation of *Cryptic* expression in the node would not be expected to affect the expression of *Nodal* in the LPM.

To ablate *Cryptic* expression in the node but leave it intact in the LPM, we rescued *Cryptic* expression specifically in the LPM of *Cryptic* knockout embryos with the use of a transgene (Fig. 3A) comprising *Cryptic* cDNA linked to IRES-*lacZ* and controlled by the LPM-specific enhancer (LPE) of *Cryptic* (Y.S., M.M.S. and H.H., unpublished) and the *hsp68* promoter. Transgenic mice that show LPM-specific expression of *lacZ* at E8.0 were established (Fig. 3B,C). These mice were then crossed with *Cryptic* mutant mice to obtain *Cryptic* knockout embryos harboring the transgene ($Cryptic^{-/-}$; Tg^+). In these embryos, *Cryptic* was expressed only in LPM (Fig. 3E), as expected, and the expression of *Nodal* in LPM was restored (6/6 embryos; Fig. 3H) to a level similar to that apparent in the wild-type embryo (Fig. 3F). Similarly, expression of the Nodal target genes (*Lefty2*, *Pitx2*) in LPM was also restored (Fig. 3L,P) to a level similar to that apparent in the wild type (Fig. 3J,N). Furthermore, the $Cryptic^{-/-}$; Tg^+ embryos were born and grew to adulthood, whereas almost all *Cryptic* knockout mice undergo neonatal death as a result of right isomeric cardiopulmonary defects

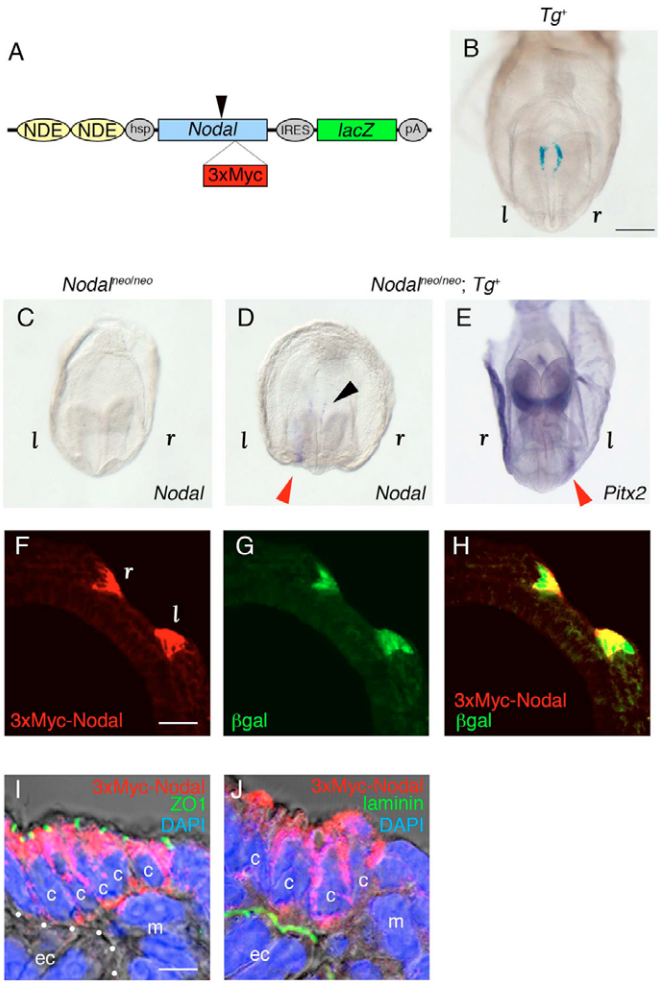

Fig. 4. Immunofluorescence detection of 3×Myc-tagged Nodal at the node. (**A**) Schematic representation of a *Nodal* transgene. Tandem node-specific enhancers (NDEs) were linked with the *hsp68* promoter, *Nodal* cDNA (encoding the 3×Myc tag positioned four amino acids downstream from the Nodal cleavage site, arrowhead), IRES, *lacZ* and pA. (**B**) An E8.2 mouse embryo harboring the transgene (*Tg*$^{+}$) exhibits β-galactosidase activity only at the node. (**C-E**) In situ hybridization for *Nodal* (C,D) or *Pitx2* (E) mRNA in *Nodal*$^{neo/neo}$ (C) or *Nodal*$^{neo/neo}$; *Tg*$^{+}$ (D,E) embryos at E8.2. The expression of the transgene (black arrowhead) rescues the loss of *Nodal* and *Pitx2* expression in LPM (red arrowheads). The level of expression of the rescued *Nodal* and *Pitx2* is lower than that in the wild-type embryo because the *neo* gene inserted into the endogenous *Nodal* gene prevents *Nodal* expression in the LPM from being amplified to the maximum level. (**F-J**) Transverse frozen sections of E8.0 *Tg*$^{+}$ embryos were subjected to immunofluorescence analysis either with antibodies to Myc (F) and to β-galactosidase (G), with the merged image shown in H, or with antibodies to Myc and to ZO-1 (I) or laminin (J), with the fluorescence signals being merged with the differential interference contrast and DAPI image (blue) in I,J. The basement membrane is indicated by white dots (I). c, crown cell of the node; ec, ectoderm; m, mesoderm. Scale bars: 200 μm in B-E; 20 μm in F-H; 5 μm in I-J.

(Yan et al., 1999). These results showed that Cryptic in the node is dispensable, with *Cryptic* expression in LPM being sufficient, for expression of *Nodal* in LPM, providing support for the direct transport model (Fig. 1B).

In a small proportion of *Cryptic*$^{-/-}$; *Tg*$^{+}$ embryos, *Nodal* (2/6 embryos) as well as the Nodal target genes were also expressed on the right side of the LPM (Fig. 3I,M,Q). Given that expression of *Lefty1* and *Lefty2* in the floor plate is absent in such embryos (Fig. 3L,M), the bilateral expression of *Nodal* is most likely due to a defect in the 'midline barrier' for Nodal (Meno et al., 1998). These results suggest that, in the absence of this barrier, Nodal produced in the left LPM is able to travel directly to the right LPM, where it activates *Nodal* expression.

Secretion of Nodal at the node

Our results indicated that Nodal produced at the node may travel from the node to the LPM via the internal route. To examine the fate of Nodal produced at the node, we generated transgenic mice that harbor a polycistronic transgene (Fig. 4A) that encodes 3×Myc-tagged Nodal and β-galactosidase and is controlled by the NDE of *Nodal* (Adachi et al., 1999). The transgenic embryos exhibited β-galactosidase activity only at the node (Fig. 4B), confirming that expression of the transgene is node-specific. The 3×Myc-Nodal protein appears to retain the functional activity of native Nodal, given that the transgene rescued the loss of *Nodal* and *Pitx2* expression in the LPM of *Nodal*$^{neo/neo}$ embryos (2/2 and 6/6 embryos, respectively; Fig. 4D,E), which lack *Nodal* expression in the node and subsequently that in LPM (Fig. 4C) (Saijoh et al., 2003). Furthermore, 3×Myc-Nodal was as active as was native Nodal in a reporter gene assay (Sakuma et al., 2002) with frog animal caps (C. Tanaka and H.H., unpublished).

Given that 3×Myc-Nodal is functional, we first investigated the subcellular localization of this protein by immunofluorescence analysis. Tight junctions and the basement membranes were visualized with antibodies to ZO-1 (Fig. 4I) and laminin (Fig. 4J), respectively, while transgene-expressing cells were detected with an antibody to β-galactosidase (Fig. 4G,H). The 3×Myc-Nodal protein was detected throughout the cytoplasm of the perinodal crown cells, not only on their apical (ventral) side but also on the lateral and basal sides adjacent to the basement membrane (Fig. 4F,H,I,J).

To examine the secretion of Nodal from the perinodal cells, we prepared immunoenzymatically stained frozen sections from the transgenic embryos (Fig. 5A-D), and ultrathin sections derived therefrom were observed by TEM (Fig. 5E-M). The 3×Myc-Nodal protein was detected specifically in the perinodal crown cells of the transgenic embryos (Fig. 5E-G), whereas no signal was detected in those of non-transgenic embryos (Fig. 5H). The staining was apparent in and around secretory vesicles, which were distributed in both the apical (Fig. 5I) and basolateral (Fig. 5J,K) regions of the perinodal cells. The staining outside the vesicles may have resulted from ultrastructural damage caused during processing of the tissue, most likely during the boiling step (Materials and methods). At higher magnification, signals were detected in the region immediately external to the basolateral (Fig. 5J-M) and apical (Fig. 5I) membranes, possibly reflecting secretion of the 3×Myc-Nodal protein. These observations suggest that Nodal produced at the node is secreted from both the apical and basolateral membranes of the perinodal crown cells. There was no apparent difference in the abundance or localization of 3×Myc-Nodal between the perinodal cells on the left and those on the right (S.O., R.H., H.O. and H.H., unpublished).

Although our results (Fig. 3) suggested that Nodal may travel from the node to LPM, 3×Myc-Nodal was detected only in or immediately external to the perinodal crown cells, with the tagged

DEVELOPMENT

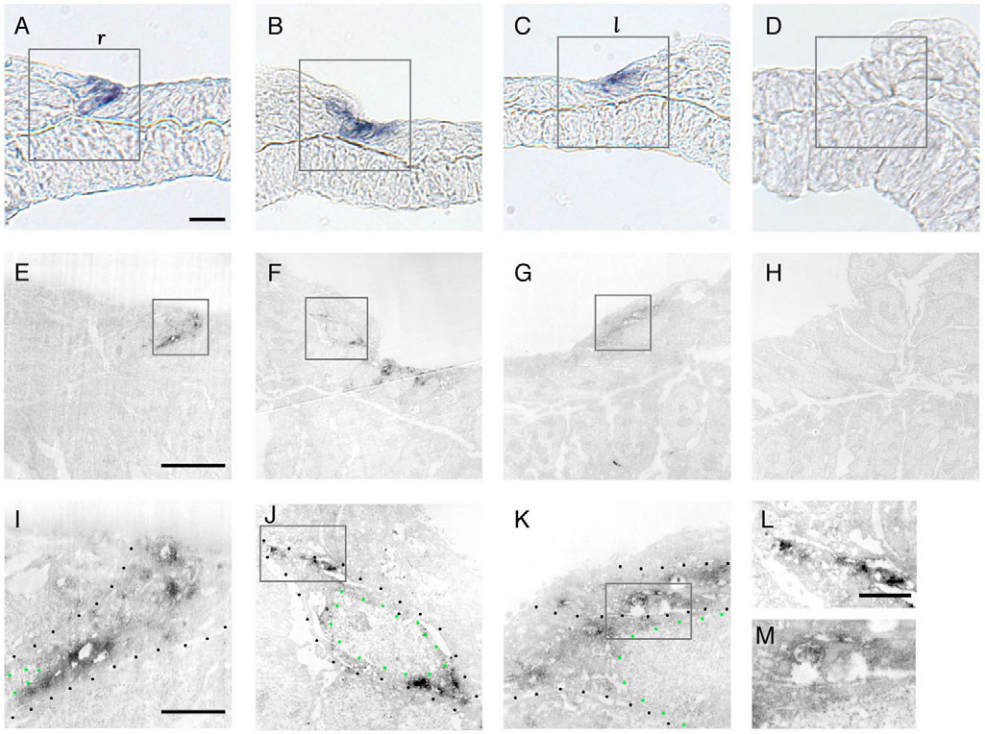

Fig. 5. Immuno-TEM detection of 3×Myc-Nodal at the node. (**A-D**) Immunohistochemical staining for 3×Myc-Nodal in transverse frozen sections of E8.0 mouse embryos positive (A-C) or negative (D) for the transgene shown in Fig. 4A. (**E-H**) Ultrathin sections corresponding to the boxed regions shown in A to D, respectively, were examined by TEM at ×1000. (**I-M**) The boxed regions in E-G are shown at higher magnification (×4000) in I-K, respectively. Black dots, cell boundaries; green dots delineate the nucleus. The boxed regions in J and K are shown at even higher magnification (×6000) in L and M, respectively, revealing apparent secretion of 3×Myc-Nodal at the basolateral membranes. Scale bars: 10 μm in A-H; 2.5 μm in I-K; 1 μm in L,M.

protein not being apparent in the region between the node and LPM. 3×Myc-Nodal traveling along the internal route, if it exists, must thus be below the limit of detection of this method.

Specific localization of sulfated GAGs between the node and LPM

Evidence (Belenkaya et al., 2004) suggests that sulfated GAGs are necessary for the long-range action of the morphogen Dpp in *Drosophila*. Although Nodal also functions over a long distance (Chen and Schier, 2001; Yamamoto et al., 2003), the possible role of GAGs in Nodal signaling has been unknown.

To examine whether GAGs might contribute to long-range signaling by Nodal from the node to the LPM, we first investigated the distribution of sulfated GAGs in the E8.0 embryo with antibodies specific for HS or for CS. Both HS and CS were localized in the basement membrane immediately below the ectoderm and endoderm layers as well as in the ECM of mesodermal cells (Fig. 6A,B). The distribution of HS and CS in the basement membrane was continuous from the node crown cells to the LPM region. Treatment of the embryo sections with heparitinase (Fig. 6D,E) or chondroitinase (Fig. 6G,H), which degrade HS and CS, respectively, resulted in a marked decrease in immunostaining for the corresponding GAG. The loss of both GAGs was induced by treatment with both enzymes (Fig. 6J,K). These results thus confirmed the specificity of the antibodies. Staining with Alcian Blue, which detects sulfated GAGs in general, also revealed a distribution pattern for these molecules similar to those apparent by immunostaining (Fig. 6C). The Alcian Blue staining remained but was reduced in intensity after treatment of sections with either heparitinase or chondroitinase (Fig. 6F,I), consistent with the previous finding that approximately equal amounts of HS and CS are present in the E8.0 embryo (Yip et al., 2002). Treatment with both enzymes resulted in a loss of Alcian Blue staining (Fig. 6L), indicating that HS and CS are the major sulfated GAGs in the E8.0 embryo.

Interaction of Nodal with sulfated GAGs

The specific distribution of sulfated GAGs between the node and the LPM (Fig. 6) suggested that Nodal may travel from the node to the LPM through interaction with sulfated GAG chains. To determine whether Nodal indeed interacts with sulfated GAGs, we incubated recombinant Nodal in vitro with heparin-sepharose beads and then subjected the beads to elution with increasing concentrations of NaCl. Most of the Nodal protein that bound to the beads was eluted by NaCl at concentrations between 0.15 and 0.90 M, a range that is higher than the physiological salt concentration, with the peak fraction corresponding to an NaCl concentration of 0.60 M (Fig. 7A). The affinity of Nodal for heparin is thus lower than that of typical heparin-binding proteins, such as heparin-binding epidermal growth factor (Takazaki et al., 2004), but it is similar to that of Dpp, which is eluted by NaCl at 0.25 to 0.40 M (Groppe et al., 1998).

To examine whether Nodal binds to various sulfated GAGs, we subjected the heparin-sepharose beads with bound Nodal to elution with graded concentrations of heparin, CS or HS (Fig. 7B). Most of the bound Nodal protein was eluted by heparin at 10 mg/ml, a

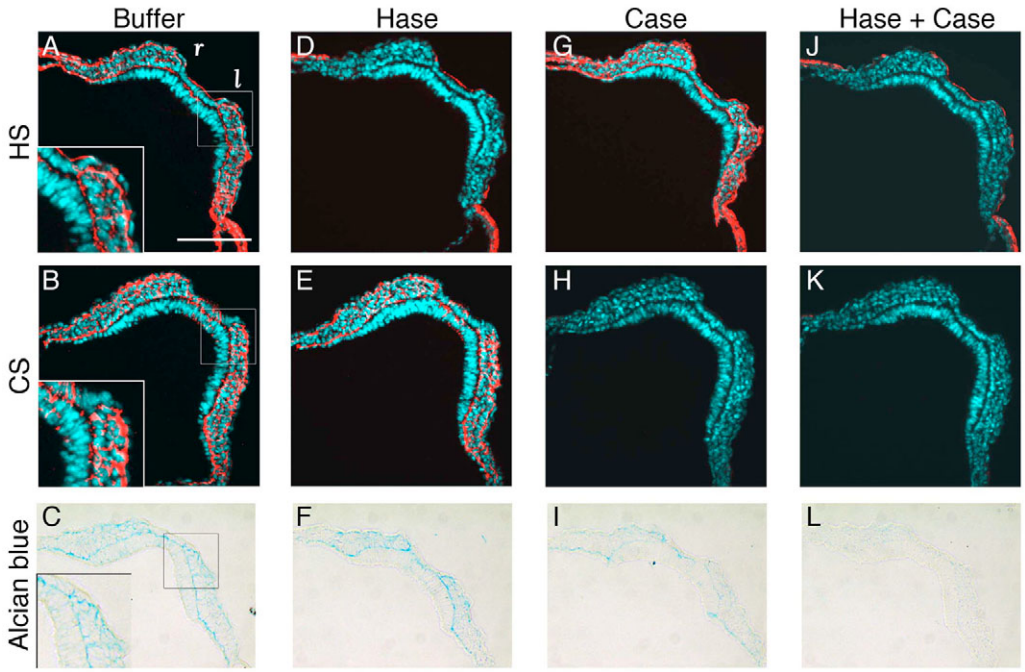

Fig. 6. Distribution of sulfated GAGs in the E8.0 mouse embryo. Transverse frozen sections of E8.0 embryos were treated with buffer only (**A-C**), heparitinase (Hase; **D-F**), chondroitinase (Case; **G-I**) or both enzymes (**J-L**) and were then subjected either to immunofluorescence analysis with antibodies to HS (10E4; A,D,G,J) or to CS (CS-56; B,E,H,K) or to staining with Alcian Blue (C,F,I,L). Red and blue indicate immunoreactivity and nuclear staining with DAPI, respectively, in the immunofluorescence images. Insets in A-C show the boxed regions at higher magnification. Scale bar: 100 μm.

concentration that is ~50 times that of heparin conjugated to the sepharose beads (10 μl beads contain ~20 μg heparin and were suspended in 100 μl elution buffer, giving a heparin concentration of ~0.2 mg/ml). Most of the bound Nodal protein was eluted by CS at 20 mg/ml, about twice the corresponding value for heparin, suggesting that the affinity of Nodal for heparin is about twice that for CS. Most of the bound Nodal protein was not eluted by HS, even at a concentration of 100 mg/ml, indicating that Nodal does not interact with HS. The failure of HS to induce Nodal elution was not due to the lower proportion of sulfate groups in HS; the relative amounts of sulfate groups per unit mass of heparin, CS or HS were about 3, 1.5 and 1, respectively [estimated by colorimetric quantitation with Toluidine Blue (S.O. and H.H., unpublished), a metachromatic reagent that stains sulfate groups of GAGs]. If the affinity is simply proportional to the amount of sulfate groups, Nodal would have been eluted by HS at 30 mg/ml. These results thus suggested that Nodal preferentially interacts with heparin and CS, but not with HS.

Asymmetric *Nodal* expression in LPM requires sulfated GAGs

We next examined whether the sulfated GAGs located specifically between the node and LPM might play a role in Nodal signal transmission between these two regions. For these experiments, we determined the effects of two agents that inhibit the synthesis of sulfated GAGs. Sodium chlorate inhibits the biosynthesis of 3′-phosphoadenosine 5′-phosphosulfate, a sulfate donor for GAG sulfation, by physically interfering with 3′-phosphoadenosine 5′-phosphosulfate synthetase, thus resulting in the production of nonsulfated GAGs rather than sulfated GAGs (Fig. 8A,J) (Greve et al., 1988; Ullrich and Huber, 2001). By contrast, *p*-nitrophenyl β-D-xylopyranoside (xyloside) acts as a primer from which GAGs are biosynthesized free from linkage to core proteins, thus resulting in the production of unlinked sulfated GAGs and naked proteoglycans (Fig. 9A,H) (Lugemwa and Esko, 1991).

If sulfated GAGs are required for transport of Nodal from the node to the LPM, inhibition of the synthesis of these molecules would be expected to result in failure of the induction of *Nodal* expression in LPM. We first determined the optimal concentrations of sodium chlorate and xyloside by culturing embryos at the headfold stage in the presence of various concentrations of each reagent until they developed to the six-somite stage. The optimal concentrations were found to be 15 mM for sodium chlorate and 1 mM for xyloside. Thus, embryos cultured with 15 mM chlorate remained morphologically normal, but the amounts of HS and CS immunoreactivity as well as the intensity of Alcian Blue staining were greatly reduced (4/4 embryos; Fig. 8K-M) in these embryos compared with those in control embryos (Fig. 8B-D). Most of the embryos cultured with 15 mM chlorate also failed to express *Nodal* in LPM, whereas normal asymmetric expression of *Nodal* was maintained at the node (Fig. 8E,N,S). The impaired expression of *Nodal* in LPM was not due to a reduced competence of LPM to respond to the Nodal signal, given that chlorate-treated embryos maintained expression of *GDF1* (4/4 embryos) and *Cryptic* (4/4 embryos) (Fig. 8F,G,O,P) and because the right LPM of the chlorate-treated embryos was able to respond to transfection with a *Nodal* expression vector (introduced together with a vector for GFP) (Nakamura et al., 2006) (12/13 embryos; Fig. 8H,I,Q,R).

Culture of embryos with 1 mM xyloside resulted in a marked reduction in the amount of CS immunoreactivity (4/4 embryos; Fig. 9C,J) but not in that of HS immunoreactivity (Fig. 9B,I). Alcian Blue

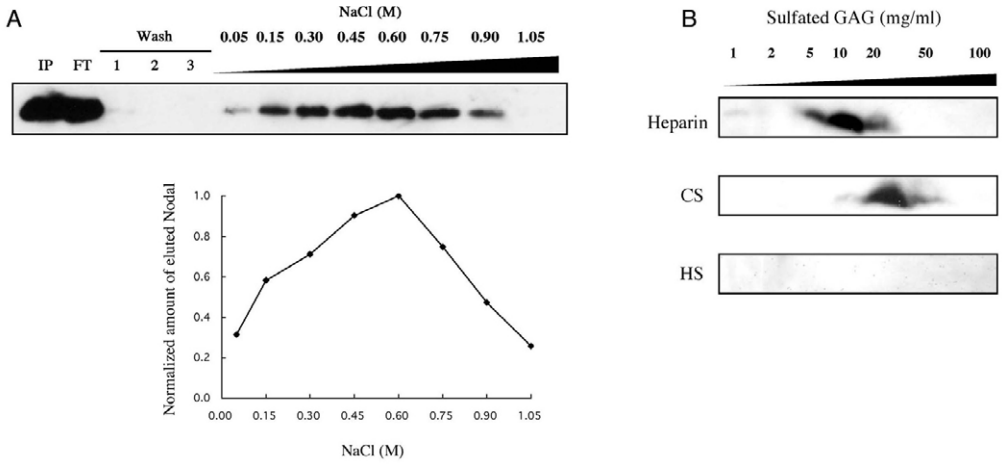

Fig. 7. Interaction of Nodal with sulfated GAGs. Recombinant mouse Nodal was incubated with heparin-sepharose beads, which were then isolated and subjected to stepwise elution with NaCl (**A**) or with heparin, CS or HS (**B**). Input (IP), flow through (FT), washed (1-3) and eluted fractions were subjected to immunoblot analysis with antibodies to Nodal. The amount of Nodal in the various fractions obtained by elution with NaCl (normalized relative to that in the fraction containing the most Nodal) was quantitated by densitometry of the immunoblot shown.

staining also remained but was slightly reduced in intensity after xyloside treatment (Fig. 9D,K). This preferential effect of xyloside on CS abundance is consistent with the previous observation that CHO cells cultured with this reagent secrete xyloside-primed CS rather than HS (Lugemwa and Esko, 1991). In the embryos cultured with xyloside, CS would thus be expected to be synthesized from the xyloside primer and secreted free of core proteins into the ECM, from which it would be washed away during culture or histological processing. Whereas asymmetric expression of *Nodal* was maintained in the node of these embryos, that in the LPM was not induced in most of them (Fig. 9E,L,Q). Similar to the results obtained with chlorate, xyloside did not affect the expression of *Cryptic* or *GDF1* (Fig. 9F,G,M,N) or the responsiveness of LPM to the Nodal signal (10/11 embryos; Fig. 9O,P).

These results indicate that the CS component of proteoglycans is necessary, whereas HS proteoglycans are not sufficient, for transmission of the Nodal signal from the node to the LPM. This CS-versus-HS specificity is consistent with our data showing that Nodal interacts preferentially with CS, not with HS (Fig. 7B).

DISCUSSION

Transport of Nodal from the node to the LPM via an internal route

Nodal flow has been suggested to transport a L-R determinant (or determinants) toward the left side (Okada et al., 2005). This notion gained support by the detection of nodal vesicular parcels (Tanaka et al., 2005). Nodal secreted from the perinodal cells toward the node cavity would be expected to be transported by the flow and might signal through the endoderm. However, we have now shown that the endoderm does not express *Cryptic* and is not responsive to the Nodal signal, making it unlikely that Nodal transported by nodal flow signals through the endoderm. A more likely scenario is that Nodal secreted basolaterally from the perinodal cells is responsible for induction of *Nodal* expression in LPM.

In the chicken embryo, the L-R signal generated at the node is transmitted to the LPM by signal relay. Thus, Sonic hedgehog produced at the node induces expression of a bone morphogenetic protein (BMP) antagonist, Caronte, which in turn activates *Nodal* expression in LPM (Yokouchi et al., 1999). However, we have now shown that Cryptic, a Nodal co-receptor essential for Nodal signaling, is dispensable in the node and is required only in the LPM for induction of *Nodal* expression in LPM. *Cryptic* is the only EGF-CFC family gene expressed in the node of E8.0 mouse embryo; *Cripto*, another member of this family, is not expressed there at this stage (see Fig. S2 in the supplementary material). These observations suggest that the Nodal signal is not relayed between the node and LPM but rather is directly transported. This notion is consistent with previous observations showing both that Nodal is able to act over a long distance (Chen and Schier, 2001; Yamamoto et al., 2003) and that asymmetric *Nodal* expression in LPM is governed by two enhancers (ASE and LSE), both of which are responsive to the Nodal signal (Saijoh et al., 2000; Saijoh et al., 2005).

How does bilateral *Nodal* expression in the node result in asymmetric *Nodal* expression in LPM?

Nodal is asymmetrically expressed exclusively in left LPM, with its bilateral expression at the node showing only a subtle L-R asymmetry. How is such a robust asymmetry generated in the LPM? If Nodal is transported from the node to LPM, is it transported preferentially toward the left side?

Although *Nodal* expression in the node exhibits a subtle asymmetry, with the level of expression on the left side being slightly higher than that on the right side, this subtle asymmetry does not appear to be essential for the robust asymmetry in LPM, because *Nodal* expression in left LPM is maintained in the transgenic embryos that express *Nodal* symmetrically at the node (Norris et al., 2002; Saijoh et al., 2003). Therefore, other genes expressed in the node with subtle asymmetry, such as *LPlunc1* and *Cerberus-like 2*, may play a role in this process (Hou et al., 2004; Marques et al., 2004; Pearce et al., 1999).

Alternatively, although *Nodal* mRNA is distributed bilaterally at the node, nodal flow may lead to the biased production of more active Nodal protein on the left side of the node. For instance, post-translational cleavage or secretion of cleaved products may occur more efficiently on the left side, in response to nodal flow. A Ca^{2+}

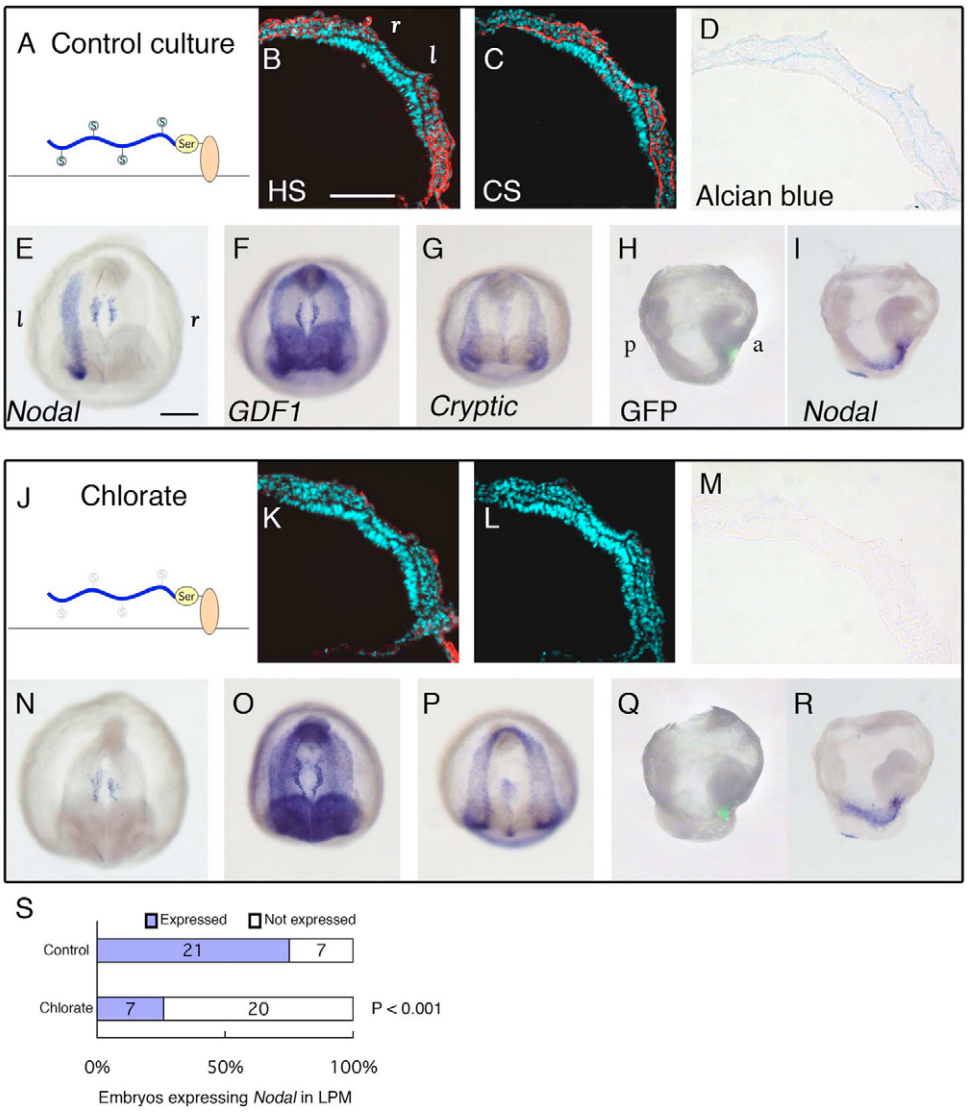

Fig. 8. Sulfated GAGs are necessary for transmission of the Nodal signal from the node to the LPM. (**A**,**J**) Schematic representation of proteoglycans from normal (A) or chlorate-treated (J) mouse embryos. A serine residue (yellow) of the core protein (orange) is attached to the GAG chain (blue curved line), which is sulfated (blue circles) under normal conditions but not in cells treated with chlorate. (**B-D**,**K-M**) Transverse frozen sections of embryos cultured to the six-somite stage in the absence (B-D) or presence (K-M) of 15 mM sodium chlorate were subjected either to immunofluorescence analysis with antibodies to HS (B,K) or to CS (C,L) or to staining with Alcian Blue (D,M). (**E-G**,**N-P**) In situ hybridization for *Nodal* (E,N), *GDF1* (F,O) or *Cryptic* (G,P) mRNAs in embryos cultured in the absence (E-G) or presence (N-P) of chlorate. (**H**,**I**,**Q**,**R**) Expression vectors for Nodal and GFP were co-injected into the right LPM of embryos at the headfold stage, which were then cultured to the six-somite stage in the absence (H,I) or presence (Q,R) of chlorate. The cultured embryos were examined for GFP fluorescence (H,Q) and then subjected to in situ hybridization for *Nodal* mRNA (I,R). It should be noted that the region of *Nodal* expression was much broader than the area expressing GFP (I,R), which is due to a competence of LPM for Nodal auto-activation. (**S**) The number and percentage of embryos with (blue) or without (white) *Nodal* expression in LPM after culture in the absence or presence of chlorate. The difference between the two culture conditions was statistically significant ($P<0.001$) by the two-tailed Fisher's exact probability test. Scale bars: 100 μm in B-D,K-M; 200 μm in E-I,N-R.

signal that exhibits asymmetry between the two sides of the node, being stronger on the left (McGrath et al., 2003), may regulate protein secretion. We did not detect a difference in the number of secretory vesicles containing Nodal between the two sides of the node (Fig. 5). However, such a difference may not necessarily be large, given that a small difference generated at the node can be autonomously converted to a robust asymmetry in LPM by a self-enhancement and lateral inhibition mechanism (Nakamura et al., 2006).

Role of sulfated GAGs in Nodal signaling

Whereas some of the many heparin-binding proteins possess a high affinity, others, such as *Drosophila* Dpp, exhibit a lower affinity (Groppe et al., 1998). Nodal was eluted from heparin-sepharose beads by NaCl most effectively at 0.45 to 0.60 M, suggesting that it possesses an intermediate affinity for heparin. Such an intermediate affinity might be expected to be ideal for transport of a protein over a long distance via sulfated GAGs (a protein with a higher affinity would become trapped by the sulfated GAGs).

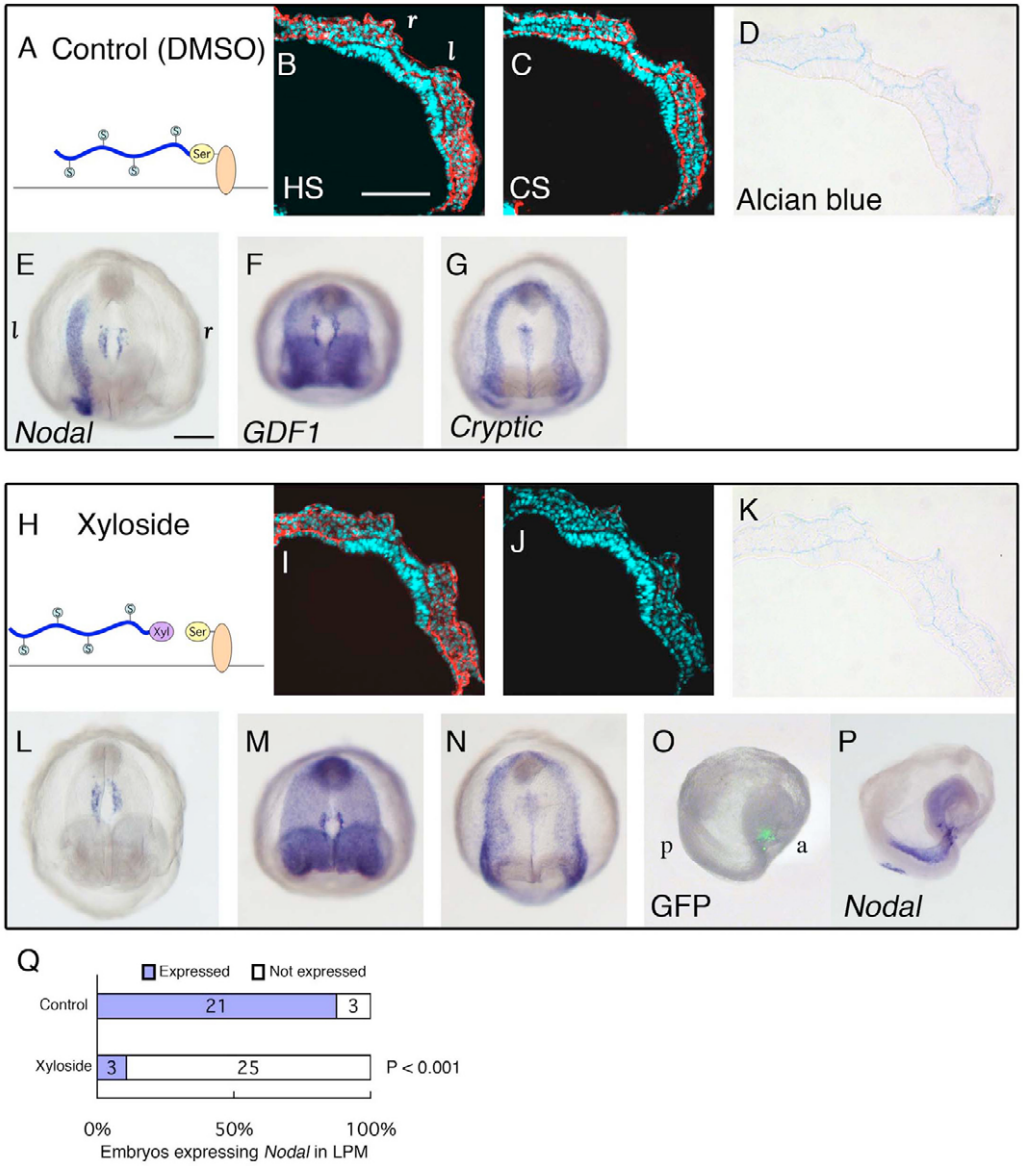

Fig. 9. CS is required for Nodal signal transmission from the node to LPM. (**A**,**H**) Schematic representation of proteoglycans from normal (A) or xyloside-treated (H) mouse embryos. Xyloside (purple) acts as primer for GAG elongation, resulting in the syntheses of unlinked GAGs and naked proteoglycans. (**B-D**,**I-K**) Transverse frozen sections of embryos cultured with 0.1% dimethyl sulfoxide vehicle (B-D) or 1 mM xyloside (I-K) to the six-somite stage were subjected either to immunofluorescence analysis with antibodies to HS (B,I) or to CS (C,J) or to staining with Alcian Blue (D,K). (**E-G**,**L-N**) In situ hybridization for *Nodal* (E,L), *GDF1* (F,M) or *Cryptic* (G,N) mRNAs in embryos cultured in the absence (E-G) or presence (L-N) of xyloside. (**O**,**P**) Expression vectors for Nodal and GFP were co-injected into the right LPM of embryos before culture with xyloside. The resulting embryos were examined for GFP fluorescence (O) and then subjected to in situ hybridization for *Nodal* mRNA (P). (**Q**) The number and percentage of embryos with (blue) or without (white) *Nodal* expression in LPM after culture in the absence or presence of xyloside. Scale bars: 100 μm in B-D,I-K; 200 μm in E-G,L-P.

The physical interaction of Nodal with sulfated GAGs, the specific localization of sulfated GAGs to the basement membrane-like structure between the node and the LPM, and the pronounced effects of inhibition of sulfated GAG synthesis observed in the present study all are consistent with a requirement for sulfated GAG chains in the efficient transport of Nodal from the node to the LPM. In *Drosophila*, Dpp is not able to move across cells deficient in HS biosynthesis (Belenkaya et al., 2004). Similarly, in the absence of sulfated GAGs, Nodal may not be transported efficiently or may become unstable. Our results suggest that CS, rather than HS, plays an important role in the long-range action of Nodal, given that Nodal interacts with CS but not with HS and that *Nodal* expression in LPM was impaired as a result of inhibition of CS proteoglycan biosynthesis by xyloside.

Sulfated GAGs have previously been implicated in L-R patterning in the frog embryo (Yost, 1990). *Xenopus* embryos treated with xyloside thus failed to undergo heart looping, a typical L-R patterning defect. Although the molecular mechanism of this effect of xyloside was not investigated, it is likely that asymmetric expression of *Xnr-1* in LPM was lost in such embryos. Furthermore, the crucial period for the xyloside effect was between stages 12 and 15, which is immediately before the

onset of asymmetric expression of *Xnr-1* in LPM and probably corresponds to the stage of the mouse embryos in our xyloside experiments. Sulfated GAGs may therefore play a role in Nodal signaling in the frog embryo similar to that demonstrated in the mouse embryo, although xyloside appears to interfere with the synthesis of HS rather than with that of CS in *Xenopus*.

To date, more than ten genes have been identified in the mouse genome that encode enzymes involved in CS biosynthesis (Silbert and Sugumaran, 2002). Two of these genes, those encoding chondroitin 6-*O*-sulfotransferases 2 and 3, have been studied by generation of mutant mice, but neither of the mutants exhibited L-R patterning defects (Uchimura et al., 2004; Uchimura et al., 2002), possibly as a result of compensation by other chondroitin 6-*O*-sulfotransferase genes. Further loss-of-function analysis of CS biosynthetic enzymes is thus required to establish the precise role of CS in Nodal signaling.

We thank H. Hashiguchi-Jo, Y. Ikawa, K. Mochida and S. Ohishi for technical assistance, and N. Mine and R. Iwamoto for experimental comments. This work was supported by grants from the Ministry of Education, Culture, Sports, Science and Technology of Japan and by CREST (H.H.), NIH (M.M.S.) and The Eccles Program in Human Molecular Biology and Genetics at University of Utah School of Medicine (Y.S.). S.O. is a recipient of a fellowship from the Japan Society for the Promotion of Science for Japanese Junior Scientists.

Supplementary material

Supplementary material for this article is available at
http://dev.biologists.org/cgi/content/full/134/21/3893/DC1

References

Adachi, H., Saijoh, Y., Mochida, K., Ohishi, S., Hashiguchi, H., Hirao, A. and Hamada, H. (1999). Determination of left/right asymmetric expression of nodal by a left side-specific enhancer with sequence similarity to a lefty-2 enhancer. *Genes Dev.* **13**, 1589-1600.

Belenkaya, T. Y., Han, C., Yan, D., Opoka, R. J., Khodoun, M., Liu, H. and Lin, X. (2004). Drosophila Dpp morphogen movement is independent of dynamin-mediated endocytosis but regulated by the glypican members of heparan sulfate proteoglycans. *Cell* **119**, 231-244.

Brennan, J., Norris, D. P. and Robertson, E. J. (2002). Nodal activity in the node governs left-right asymmetry. *Genes Dev.* **16**, 2339-2344.

Chen, Y. and Schier, A. F. (2001). The zebrafish Nodal signal Squint functions as a morphogen. *Nature* **411**, 607-610.

Garcia-Garcia, M. J. and Anderson, K. V. (2003). Essential role of glycosaminoglycans in Fgf signaling during mouse gastrulation. *Cell* **114**, 727-737.

Greve, H., Cully, Z., Blumberg, P. and Kresse, H. (1988). Influence of chlorate on proteoglycan biosynthesis by cultured human fibroblasts. *J. Biol. Chem.* **263**, 12886-12892.

Groppe, J., Rumpel, K., Economides, A. N., Stahl, N., Sebald, W. and Affolter, M. (1998). Biochemical and biophysical characterization of refolded Drosophila DPP, a homolog of bone morphogenetic proteins 2 and 4. *J. Biol. Chem.* **273**, 29052-29065.

Hacker, U., Nybakken, K. and Perrimon, N. (2005). Heparan sulphate proteoglycans: the sweet side of development. *Nat. Rev. Mol. Cell Biol.* **6**, 530-541.

Hamada, H., Meno, C., Watanabe, D. and Saijoh, Y. (2002). Establishment of vertebrate left-right asymmetry. *Nat. Rev. Genet.* **3**, 103-113.

Hirose, H., Shirota, K. and Makita, T. (1990). Ultra grids for observation of same wide specimen at low and high magnification. In *Proceedings of the 12th International Congress for Electron Microscopy* (ed. L. D. Peachy and D. B. Williams), pp. 728-729. Seattle, San Francisco: San Francisco Press.

Hou, J., Yashiro, K., Okazaki, Y., Saijoh, Y., Hayashizaki, Y. and Hamada, H. (2004). Identification of a novel left-right asymmetrically expressed gene in the mouse belonging to the BPI/PLUNC superfamily. *Dev. Dyn.* **229**, 373-379.

Lin, X. (2004). Functions of heparan sulfate proteoglycans in cell signaling during development. *Development* **131**, 6009-6021.

Lowe, L. A., Supp, D. M., Sampath, K., Yokoyama, T., Wright, C. V., Potter, S. S., Overbeek, P. and Kuehn, M. R. (1996). Conserved left-right asymmetry of nodal expression and alterations in murine situs inversus. *Nature* **381**, 158-161.

Lugemwa, F. N. and Esko, J. D. (1991). Estradiol beta-D-xyloside, an efficient primer for heparan sulfate biosynthesis. *J. Biol. Chem.* **266**, 6674-6677.

Marques, S., Borges, A. C., Silva, A. C., Freitas, S., Cordenonsi, M. and Belo, J. A. (2004). The activity of the Nodal antagonist Cerl-2 in the mouse node is required for correct L/R body axis. *Genes Dev.* **18**, 2342-2347.

McGrath, J., Somlo, S., Makova, S., Tian, X. and Brueckner, M. (2003). Two populations of node monocilia initiate left-right asymmetry in the mouse. *Cell* **114**, 61-73.

Meno, C., Saijoh, Y., Fujii, H., Ikeda, M., Yokoyama, T., Yokoyama, M., Toyoda, Y. and Hamada, H. (1996). Left-right asymmetric expression of the TGF beta-family member lefty in mouse embryos. *Nature* **381**, 151-155.

Meno, C., Ito, Y., Saijoh, Y., Matsuda, Y., Tashiro, K., Kuhara, S. and Hamada, H. (1997). Two closely-related left-right asymmetrically expressed genes, lefty-1 and lefty-2: their distinct expression domains, chromosomal linkage and direct neuralizing activity in Xenopus embryos. *Genes Cells* **2**, 513-524.

Meno, C., Shimono, A., Saijoh, Y., Yashiro, K., Mochida, K., Ohishi, S., Noji, S., Kondoh, H. and Hamada, H. (1998). lefty-1 is required for left-right determination as a regulator of lefty-2 and nodal. *Cell* **94**, 287-297.

Morriss-Kay, G. M. and Crutch, B. (1982). Culture of rat embryos with beta-D-xyloside: evidence of a role for proteoglycans in neurulation. *J. Anat.* **134**, 491-506.

Nakamura, T., Mine, N., Nakaguchi, E., Mochizuki, A., Yamamoto, M., Yashiro, K., Meno, C. and Hamada, H. (2006). Generation of robust left-right asymmetry in the mouse embryo requires a self-enhancement and lateral-inhibition system. *Dev. Cell* **11**, 495-504.

Norris, D. P., Brennan, J., Bikoff, E. K. and Robertson, E. J. (2002). The Foxh1-dependent autoregulatory enhancer controls the level of Nodal signals in the mouse embryo. *Development* **129**, 3455-3468.

Okada, Y., Takeda, S., Tanaka, Y., Belmonte, J. C. and Hirokawa, N. (2005). Mechanism of nodal flow: a conserved symmetry breaking event in left-right axis determination. *Cell* **121**, 633-644.

Pearce, J. J., Penny, G. and Rossant, J. (1999). A mouse cerberus/Dan-related gene family. *Dev. Biol.* **209**, 98-110.

Rankin, C. T., Bunton, T., Lawler, A. M. and Lee, S. J. (2000). Regulation of left-right patterning in mice by growth/differentiation factor-1. *Nat. Genet.* **24**, 262-265.

Saijoh, Y., Adachi, H., Sakuma, R., Yeo, C. Y., Yashiro, K., Watanabe, M., Hashiguchi, H., Mochida, K., Ohishi, S., Kawabata, M. et al. (2000). Left-right asymmetric expression of lefty2 and nodal is induced by a signaling pathway that includes the transcription factor FAST2. *Mol. Cell* **5**, 35-47.

Saijoh, Y., Oki, S., Ohishi, S. and Hamada, H. (2003). Left-right patterning of the mouse lateral plate requires nodal produced in the node. *Dev. Biol.* **256**, 160-172.

Saijoh, Y., Oki, S., Tanaka, C., Nakamura, T., Adachi, H., Yan, Y. T., Shen, M. M. and Hamada, H. (2005). Two nodal-responsive enhancers control left-right asymmetric expression of Nodal. *Dev. Dyn.* **232**, 1031-1036.

Sakuma, R., Ohnishi Yi, Y., Meno, C., Fujii, H., Juan, H., Takeuchi, J., Ogura, T., Li, E., Miyazono, K. and Hamada, H. (2002). Inhibition of Nodal signalling by Lefty mediated through interaction with common receptors and efficient diffusion. *Genes Cells* **7**, 401-412.

Shen, M. M., Wang, H. and Leder, P. (1997). A differential display strategy identifies Cryptic, a novel EGF-related gene expressed in the axial and lateral mesoderm during mouse gastrulation. *Development* **124**, 429-442.

Shiratori, H. and Hamada, H. (2006). The left-right axis in the mouse: from origin to morphology. *Development* **133**, 2095-2104.

Silbert, J. E. and Sugumaran, G. (2002). Biosynthesis of chondroitin/dermatan sulfate. *IUBMB Life* **54**, 177-186.

Takazaki, R., Shishido, Y., Iwamoto, R. and Mekada, E. (2004). Suppression of the biological activities of the epidermal growth factor (EGF)-like domain by the heparin-binding domain of heparin-binding EGF-like growth factor. *J. Biol. Chem.* **279**, 47335-47343.

Tanaka, Y., Okada, Y. and Hirokawa, N. (2005). FGF-induced vesicular release of Sonic hedgehog and retinoic acid in leftward nodal flow is critical for left-right determination. *Nature* **435**, 172-177.

Uchimura, K., Kadomatsu, K., Nishimura, H., Muramatsu, H., Nakamura, E., Kurosawa, N., Habuchi, O., El-Fasakhany, F. M., Yoshikai, Y. and Muramatsu, T. (2002). Functional analysis of the chondroitin 6-sulfotransferase gene in relation to lymphocyte subpopulations, brain development, and oversulfated chondroitin sulfates. *J. Biol. Chem.* **277**, 1443-1450.

Uchimura, K., Kadomatsu, K., El-Fasakhany, F. M., Singer, M. S., Izawa, M., Kannagi, R., Takeda, N., Rosen, S. D. and Muramatsu, T. (2004). N-acetylglucosamine 6-O-sulfotransferase-1 regulates expression of L-selectin ligands and lymphocyte homing. *J. Biol. Chem.* **279**, 35001-35008.

Ullrich, T. C. and Huber, R. (2001). The complex structures of ATP sulfurylase with thiosulfate, ADP and chlorate reveal new insights in inhibitory effects and the catalytic cycle. *J. Mol. Biol.* **313**, 1117-1125.

Yamamoto, M., Mine, N., Mochida, K., Sakai, Y., Saijoh, Y., Meno, C. and Hamada, H. (2003). Nodal signaling induces the midline barrier by activating Nodal expression in the lateral plate. *Development* **130**, 1795-1804.

Yan, Y. T., Gritsman, K., Ding, J., Burdine, R. D., Corrales, J. D., Price, S. M., Talbot, W. S., Schier, A. F. and Shen, M. M. (1999). Conserved requirement for EGF-CFC genes in vertebrate left-right axis formation. *Genes Dev.* **13**, 2527-2537.

Yip, G. W., Ferretti, P. and Copp, A. J. (2002). Heparan sulphate proteoglycans and spinal neurulation in the mouse embryo. *Development* **129**, 2109-2119.
Yokouchi, Y., Vogan, K. J., Pearse, R. V., 2nd and Tabin, C. J. (1999). Antagonistic signaling by Caronte, a novel Cerberus-related gene, establishes left-right asymmetric gene expression. *Cell* **98**, 573-583.
Yost, H. J. (1990). Inhibition of proteoglycan synthesis eliminates left-right asymmetry in Xenopus laevis cardiac looping. *Development* **110**, 865-874.

DEVELOPMENT